Steady-State Kinetics of Substrate Binding and Iron Release in Tomato ACC Oxidase†

Julia S. Thrower, Richard Blalock III,§ and Judith P. Klinman*

Departments of Chemistry and of Molecular and Cell Biology, University of California, Berkeley, Berkeley, California 94720-1460

Received February 15, 2001; Revised Manuscript Received May 18, 2001

ABSTRACT: 1-Aminocyclopropane-1-carboxylate oxidase (ACC oxidase) catalyzes the last step in the biosynthetic pathway of the plant hormone, ethylene. This unusual reaction results in the oxidative ring cleavage of 1-aminocyclopropane carboxylate (ACC) into ethylene, cyanide, and CO_2 and requires ferrous ion, ascorbate, and molecular oxygen for catalysis. A new purification procedure and assay method have been developed for tomato ACC oxidase that result in greatly increased enzymatic activity. This method allowed us to determine the rate of iron release from the enzyme and the effect of the activator, CO_2, on this rate. Initial velocity studies support an ordered kinetic mechanism where ACC binds first followed by O_2; ascorbate can bind after O_2 or possibly before ACC. This kinetic mechanism differs from one recently proposed for the ACC oxidase from avocado.

Ethylene, one of the first identified endogenous chemical regulators in plants, functions as a signal for a number of biological processes such as seed germination, senescence, and fruit ripening (*1*). 1-Aminocyclopropane-1-carboxylate oxidase (ACC oxidase) catalyzes the last step in the ethylene biosynthetic pathway: the two electron oxidation of 1-aminocyclopropane-1-carboxylic acid (ACC)[1] to ethylene, carbon dioxide, and cyanide (*2*). This reaction also requires the concomitant reduction of molecular oxygen to two equivalents of water and the oxidation of ascorbate to dehydroascorbate (*3*). ACC oxidase belongs to a rapidly growing family of mononuclear nonheme iron enzymes that are characterized by a 2-histidine-1-carboxylic acid (2H-1C) iron-binding motif (reviewed in ref *4*). Within this class, a variety of reactions are catalyzed, such as hydroxylations [e.g., prolyl hydroxylase; *5*], oxidative ring closures [e.g., isopenicillin N. synthase; reviewed in ref *6*], ring expansions [e.g., deacetoxycephalosporin C synthase; *7*], and desaturations [e.g., clavaminate synthase; *8*]. The mechanistic understanding of how a class of enzymes with similar active sites can catalyze such a wide range of reactions is poor.

We have undertaken studies of ACC oxidase from tomato, with the goal of performing mechanistic studies on the unusual ring cleavage reaction that leads to ethylene, CO_2, and HCN (Scheme 1). These studies have led to a new enzyme purification procedure and assay method that give greatly increased activity. We also present an enzyme trapping method that allows the rate of Fe(II) release from the enzyme to be determined both in the absence and presence of the activator, CO_2. Finally, from initial rate studies, we arrive at a kinetic mechanism for tomato ACC oxidase that differs from one recently proposed for the ACC oxidase from avocado (*9*).

Scheme 1

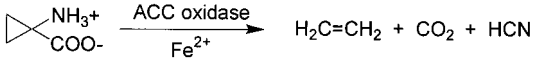

EXPERIMENTAL PROCEDURES

Materials. Sodium L-ascorbate and ACC were purchased from Aldrich. All other reagents were purchased from Sigma unless otherwise indicated.

Overexpression and Purification. The gene for ACC oxidase from *Lycopersicon esculentum* (ACO1) was obtained from A. Hamilton on a T7-T3 alpha plasmid (*10*). Plasmid pET3a-ACO1 was generated by standard procedures. ACC oxidase was produced in *Escherichia coli* strain BL21(DE3)-pLysS. Cells (6 L) were grown at 37 °C in media containing 100 μg/mL each of ampicillin and choramphenicol to an $OD_{600} \sim 1$. The temperature was shifted down to 27 °C and an additional amount of ampicillin and choramphenicol were added, along with isopropyl-β-D-galactopyranoside (0.2 mM). After 2 h, cells were harvested by centrifugation at 5000 rpm (SS34), frozen −80 °C, and thawed in 25 mM HEPES, pH 8.0, 1 mM EDTA, 5 mM DTT, 10% glycerol, and 1 μg/mL lysozyme. Lysis proceeded for 20−30 min after which the cell pellet was fully resuspended and the suspension was viscous. DNAse I (10 U/mL) and $MgCl_2$ (5 mM) were added to digest the DNA. The lysate was centrifuged

† Supported by a grant (to J.P.K.) from the NIH (GM 25765).

* To whom correspondence should be addressed. Department of Chemistry, University of California, Berkeley, Berkeley, CA 94720-1460. Phone: (510) 642-2668. Fax: (510) 643-6232. E-mail: klinman@socrates.berkeley.edu.

§ Present address: Department of Chemistry, Morehouse College, Atlanta, GA 30365.

[1] Abbreviations: ACC, 1-aminocyclopropane-1-carboxylic acid; Asc, ascorbate; BSA, bovine serum albumin; DTT, dithiothreitol; EDTA, ethylenediaminetetraacetic acid; HEPES, *N*-(2-hydroxyethyl)piperizine-*N*′-(2-ethanesulfonic acid); 2H-1C, 2-histidine-1-carboxylic acid; MOPS, 3-(*N*-morpholino)propanesulfonic acid; PAGE, polyacrylamide gel electrophoresis; SDS, sodium dodecyl sulfate; ICP, inductively coupled plasma.

10.1021/bi010329c CCC: $20.00
Published on Web 07/21/2001

at 8000 rpm (SS34) at 4 °C for 20 min, and NaCl (25 mM) was added to the supernatant. The supernatant was loaded onto Q-Sepharose resin (Amersham Pharmacia) equilibrated with buffer A (25 mM HEPES, pH 8.0, 1.0 mM EDTA, 5 mM DTT, 25 mM NaCl, and 10% glycerol). The column was washed with buffer A containing 50 mM NaCl. ACC oxidase was eluted with buffer A containing 100 mM and then 150 mM NaCl. One peak eluted at each NaCl concentration. These were concentrated separately in a Ultrafree concentrator 10K MWCO (Millipore), and peak 1 was further purified on Superdex 75 gel filtration resin (Amersham Pharmacia) equilibrated in 25 mM HEPES, pH 8.0, 10% glycerol. ACC oxidase, peak 1, was ~95% pure as determined by sodium dodecyl sulfate−polyacrylamide gel electrophoresis (SDS−PAGE). Protein concentration was determined by Bradford assay using bovine serum albumin (BSA) as a standard. Peak 2 was found to be completely inactive. Iron concentration in the protein was determined by ICP analysis.

Initial Velocity Assays. Initial velocities were measured by the rate of oxygen consumption at 25 °C, pH 7.2, using an YSI model 5300 biological oxygen monitor. Temperature was maintained at 25 ± 0.1 °C with a Neslab circulating water bath. Standard reaction mixture (1 mL) contained 100 mM MOPS, pH 7.2, 20 mM $NaHCO_3$, 100 mM NaCl, 2 mM DTT, 0.1 mg/mL BSA, 0.1 mg/mL catalase, and various amounts of ascorbate and ACC. When ACC and ascorbate were kept constant, concentrations were maintained at 0.5 and 25 mM, respectively. Each reaction mixture was made from stock solutions by addition of concentrated solutions of ascorbate, catalase, and ACC. When the oxygen concentration was varied, the reaction mixture was equilibrated by stirring for at least 10 min with the appropriate premixed O_2/N_2 gas mixture to obtain the desired oxygen concentration. Starting oxygen concentrations were determined using the oxygen monitor that was calibrated with air saturated water (258 μM oxygen at 25 °C). Reactions were initiated with 2 μL of ACC oxidase reconstituted with equimolar $Fe(NH_4)_2(SO_4)_2$. Because of the loss of activity upon prolonged exposure to Fe(II) in the presence of oxygen, ACC oxidase was reconstituted in small aliquots and used within 30 min. Concentration of ACC oxidase is as indicated in figure legends. All initial rates were measured under conditions where less than 5% of any given substrate was consumed. All rates were calculated subtracting background oxygen consumption due to ascorbate and/or Fe(II) in the absence of enzyme. Data from initial velocity experiments with varying substrate concentrations were fitted to eq 1 using the program Kaleidagraph.

$$\nu = \frac{V_{max}[S]}{K + [S]} \quad (1)$$

Dissociation Constant for Iron. The dissociation constant, K_d, for Fe(II) was determined by injecting 2 μL of apo-ACC oxidase into the standard reaction mixture containing varying concentrations of $Fe(NH_4)_2(SO_4)_2$. Activity was measured by oxygen consumption as described above. For each reaction, the background rate of oxygen consumption due to reaction with Fe(II) and ascorbate was subtracted. The double reciprocal plot of initial velocity vs Fe(II) concentration showed curvilinear behavior. Data were fitted to eq 2 using the program Kaleidagraph (see appendix).

$$\nu = \frac{V_{max}}{1 + \frac{K_d}{[Fe]_t - \frac{K_d + [Fe]_t + [E]_t - \sqrt{(-[E]_t - [Fe]_t - K_d)^2 - 4[E]_t[Fe]_t}}{2}}} \quad (2)$$

Dissociation Rate Constant for Iron. Dissociation rate constants for Fe(II) were determined by diluting 2 μL of holo-ACC oxidase (≥180 μM) into the standard reaction mixture containing 25 μM $ZnCl_2$ (but without ascorbate and ACC) and either 20 mM $NaHCO_3$ or no additional $NaHCO_3$. After time, *t*, activity was measured by injecting 2 μL of 0.25 M ACC, 1.6 M ascorbate solution into reactions containing added $NaHCO_3$, or 2 μL of 0.25 M ACC, 1.6 M ascorbate, 0.2 M $NaHCO_3$ solution into reactions without $NaHCO_3$. Since background oxygen consumption due to ascorbate cannot be directly measured for each assay, an average background rate of oxygen consumption in the absence of enzyme (average of three measurements) was subtracted from initial rate. Activity at any given time represents fraction of holo-ACC oxidase remaining relative to activity at $t = 0$. Data were fitted to eq 3 using the program Kaleidagraph.

$$\frac{[E(Fe)]}{[Et]} = Ae^{(-k_{obs}t)} + C \quad (3)$$

RESULTS

Enzyme Purification. A protocol was developed that is a modification of that reported by Barlow et al. (*11*). Previous procedures used a linear NaCl gradient to elute recombinant ACC oxidase from a Q-sepharose column. In our hands, we found that most of the *Escherichia coli* proteins coeluted with ACC oxidase, making purification by this method inefficient. Using a NaCl step gradient, rather than a linear gradient, during purification from Q-sepharose resin not only resulted in superior separation of most *E. coli* proteins from ACC oxidase, but also in the elution of ACC oxidase as two distinct peaks at 100 mM (peak 1) and 150 mM NaCl (peak 2) that are attributed to ACC oxidase based on their molecular weight determination on SDS−PAGE (data not shown). Peak 1 was further purified from a gel filtration column to yield protein that was ~95% pure as determined by SDS−PAGE analysis (data not shown). This peak, estimated as ~75% of total soluble ACC oxidase from the sum of peaks 1 and 2 (~200 mg), was active when added to the reaction mixture (as described in Experimental Procedures) containing 600 nM ACC oxidase and 5 μM Fe(II) with $k_{obs} = 19.7$ min^{-1}, which is 7- to 40-fold more active than previously reported values of 0.5−3 min^{-1} in the presence of ≥ 5 μM Fe(II) (*12*, *13*). Initial rates were linear for > 10 min, consistent with previous reports [data not shown and ref *14*]. In contrast to peak 1, peak 2 showed no activity in the presence of Fe(II) (data not shown). Neither purified peak contained any detectable amounts of iron above background as determined by ICP analysis (data not shown).

Kinetics of Holo-ACC Oxidase. Although ACC oxidase has been reported to contain a single bound Fe(II) molecule per monomer, assays typically require a large molar excess

Table 1: Kinetic Parameters for ACC Oxidase[a]

param	Fe(II)	ACC	ascorbate	O_2
V_{max}(min^{-1})	22.3 ± 0.4	26.7 ± 1.3	31.0 ± 1.7	23.1 ± 0.4
K_m		76.9 ± 9.7 μM	4.64 ± 0.64 mM	28.2 ± 2.0 μM
K_d[b]	0.50 ± 0.04 μM			
K_i[c]		38.9 ± 9.4 mM		

[a] Kinetic parameters were determined by measuring initial velocities at various concentrations of one substrate while maintaining the other substrates at a constant concentration. Constant concentrations were [ACC] = 0.5 mM, [ascorbate] = 20 mM, or [O_2] = 258 μM. [b] Determined in the presence of 20 mM CO_2/bicarbonate. [c] K_i for ACC was determined in the presence of 5 mM ascorbate.

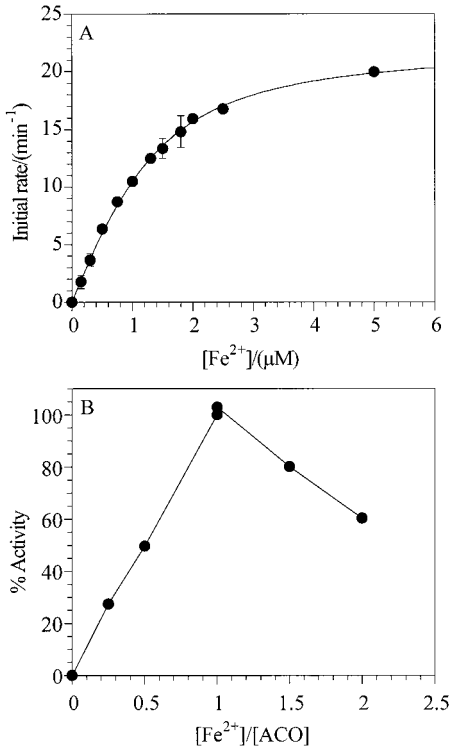

FIGURE 1: Activity of ACC oxidase in the presence of excess or stoichiometric Fe(II). (A) Dependence of the rate on Fe(II) concentration added to reaction mixture. [ACC oxidase] = 1.2 μM. (B) Stoichiometry of Fe(II) required for maximal activity. Final [ACC oxidase] = 0.3 μM in the assay.

of iron (over 10-fold more iron than enzyme) to reach maximal activity (*12*, *13*). We determined the requirement of iron for maximal ACC oxidase activity by comparing two different assay methods. Reactions were performed either by diluting apo-ACC oxidase into an assay mixture containing Fe(II) or preincubating ACC oxidase with Fe(II) to form holo-ACC oxidase and then diluting into an assay mixture without additional Fe(II).

To determine the dependence of the initial velocity on the Fe(II) concentrations, the first method was used (final ACC oxidase concentration = 1.2 μM) in the presence of 0−5 μM Fe(II) (Figure 1a). Reaction time courses were linear for >5 min. The lack of a linear dependence of the initial rate on the concentration of Fe(II) up to an amount stoichiometric with enzyme rules out very tight binding of metal. No inhibition was seen with Fe(II) concentrations up to 5 μM. The data were fit to a quadratic equation (eq 2 in Experimental Procedures) with a corresponding dissociation constant for iron, K_d, of 0.50 ± 0.04 μM (Table 1). This K_d is similar to previously reported K_m values for apple ACC oxidase [1 μM; *15*] and to other 2H-1C iron-binding enzymes, such as prolyl hydroxylase [2 μM; *16*].

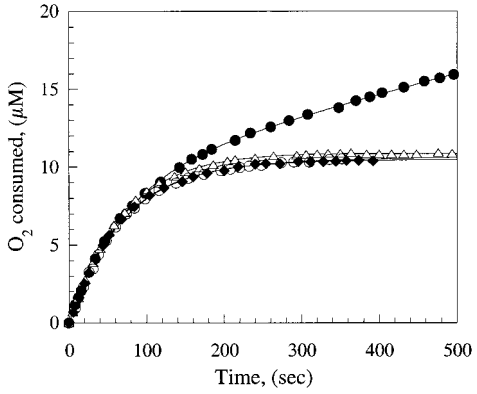

FIGURE 2: Zn(II) affects the time course of the ACC oxidase reaction. Holo-ACC oxidase reaction time course in the presence of 0 (●), 5 μM (Δ), 10 μM (○), and 50 μM (♦) zinc. Final [ACC oxidase] = 0.3 μM in the assay. The rate of O_2 consumption was fit with a first-order single-exponential equation, giving k_{obs} for all plots = 0.014−0.015 s^{-1}.

To determine the stoichiometry of iron required to give maximal activity, the second assay method was used. Apo-ACC oxidase was first preincubated with various concentrations of Fe(II). To ensure maximum complex formation between metal and enzyme, the concentration of ACC oxidase (≥ 150 μM) was maintained well above the K_d value for Fe(II) in the preincubation mixture. The activity was then determined by diluting holo-ACC oxidase 500-fold into a reaction mixture that contained ascorbate and ACC (Figure 1b). Initial rates increased proportionally with the amount of Fe(II) added up to equimolar amounts. However, reconstitution with progressively excess Fe(II) led to a decrease in the initial rate. The decrease in rate appears to correlate in approximately linear fashion with the amount of excess Fe(II). It is uncertain whether this represents the presence of a low affinity allosteric iron binding site, or arises from damage to the enzyme by oxidizing species that form from reaction of iron and O_2 in solution. In contrast to the reactions initiated with apo-ACC oxidase, initial velocities were linear for only ∼50 s, after which the rate decreased until it reached a second equilibrium rate (Figure 2, solid circles). This second phase was linear for >5 min. The behavior of the time course is consistent with the loss of activity being due to Fe(II) release from the enzyme over time until a new equilibrium level of holo-ACC oxidase and free Fe(II) is reached.

Effect of CO_2 on ACC Oxidase Kinetics. ACC oxidase activity is dependent on the presence of HCO_3^-/CO_2 in solution (*13*, *17*, *18*). The mechanism of activation is not yet understood. To determine whether activation by HCO_3^-/CO_2 occurred by the same pathway whether the reaction was initiated with apo-ACC oxidase or with holo-ACC oxidase, we compared the amount of activation in the presence of

Scheme 2

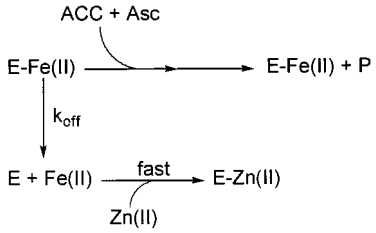

saturating bicarbonate [20 mM, corresponding to 3.3 mM CO_2 at pH 7.2; *17*] and ambient conditions (1.1 μM HCO_3^-, 0.15 μM CO_2 in solution at pH 7.2). Independent of the assay method, addition of bicarbonate increased the rate of the reaction ~5.5-fold relative to that of ambient conditions (data not shown).

Fernández-Maculet et al. provided evidence that CO_2 rather than bicarbonate is the true activator (*18*). In support of evidence that CO_2 is the activating species, we find that the bisulfite ion (isoelectronically similar to bicarbonate) is unable to stimulate ACC oxidase activity (data not shown).

Measurement of Fe(II) Release. To determine the rate of Fe(II) release, an enzyme-trapping method was developed (Scheme 2). In this method, an alternative metal is used to prevent rebinding of Fe(II) once it dissociates from the enzyme. Not only is it critical that the alternative metal bind rapidly and tightly to the enzyme, but it must be inactive in enzymatic turnover or partial reactions involving redox chemistry with oxygen. The nonredox metal, Zn(II), was previously shown to be an effective inhibitor of ACC oxidase activity, eliminating at least 96% of activity when combined in an assay with equimolar Fe(II) (*14*). To determine whether zinc would function as an "enzyme trap," we monitored the time course of a reaction initiated with holo-ACC oxidase in the presence of 0−50 μM $ZnCl_2$ (Figure 2). Identical initial rates (where all enzyme is in complex with Fe(II)) in the presence or absence of zinc provide evidence that zinc does not inhibit by binding at a nonspecific site(s) on the enzyme. In the absence of zinc, the time course showed the characteristic decrease in rate to a final linear phase, which lasted >5 min (Figure 2, solid circles). In the presence of even the lowest concentration of zinc (5 μM) the time course came to a plateau level with a final rate of zero, indicating complete inhibition of ACC oxidase. Further increase in zinc concentrations showed no change in the reaction kinetics. From these data, a K_d for zinc is estimated to be < 0.2 μM. From the plateau level of oxygen consumed, ACC oxidase undergoes an average of 33 turnovers before Fe(II) dissociates from the active site.

To measure the rate of Fe(II) release, ACC oxidase was preincubated at high concentrations (150 μM) with an equimolar amount of Fe(II) to ensure complete binding. Reconstituted ACC oxidase was diluted 500-fold into buffer containing an excess amount of zinc. After a given time, the fraction of holo-ACC oxidase remaining was determined by measuring activity after injecting substrates. The rate of Fe(II) release was determined in both the presence of saturating CO_2 and ambient CO_2 conditions (Figure 3). The data were fit to a first-order single-exponential equation (eq 3 in Experimental Procedures). The presence of saturating CO_2 (k_{off} = 0.033 ± 0.003 s^{-1}) resulted in a ca. 2-fold decrease in the rate of Fe(II) release as compared to ambient

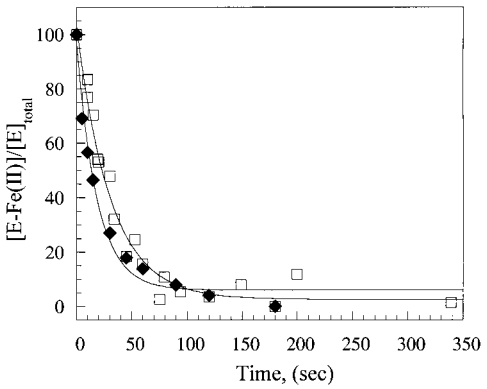

FIGURE 3: Effect of CO_2 on the rate of Fe(II) release from ACC oxidase. Dissociation rate constant for Fe(II) in the presence of ambient (□) or 20 mM (♦) HCO_3^-/CO_2. k_{off} (ambient) = 0.058 ± 0.005 s^{-1}. k_{off} (20 mM HCO_3^-/CO_2) = 0.033 ± 0.003 s^{-1}. Final [ACC oxidase] = 0.6 μM in the assay.

conditions (k_{off} = 0.058 ± 0.005 s^{-1}). From the experimentally determined K_d and k_{off} values, the rate of association of Fe(II) can be calculated from the relationship $K_d = k_{off}/k_{on}$, giving a value for k_{on} of 6.6 × 10^4 M^{-1} s^{-1} at saturating CO_2. In contrast to ACC oxidase activity at saturating CO_2 concentrations, the low activity when measured at ambient CO_2 precluded the determination of a K_d value and, hence, k_{on} for iron under such conditions.

Kinetic Mechanism. Steady-state kinetic parameters, shown in Table 1, were obtained by maintaining two substrates at high concentrations (see Table 1) while determining the dependence of the initial velocity on the concentration of the third substrate. Values of K_m for all substrates are similar to those previously reported for enzyme from apple (*18*), avocado (*14*), tomato (*19*), and melon (*20*). Values for k_{cat} = 25−30 min^{-1} are identical whether assays were initiated with apo-ACC oxidase or holo-ACC oxidase and, as noted above, are 7- to 40-fold higher than previously reported (*12*, *13*).

Slight inhibition by high concentrations of ACC in the presence of "optimal" concentrations of oxygen and ascorbate was previously shown with avocado ACC oxidase (*9*). Although we did not observe inhibition by ACC under similar conditions (data not shown), high concentrations of ACC did inhibit the reaction when ascorbate was maintained at concentrations close to the K_m value ($K_{i(ACC)}$ = 38.9 ± 9.4 mM, Table 1). In no case was inhibition by high ascorbate concentrations (≤30 mM) seen. Oxygen was kept constant at 258 μM for all substrate inhibition experiments.

To determine the steady-state kinetic mechanism of substrate binding, initial velocity patterns were obtained for ACC, ascorbate, or oxygen as the varied substrate. Substrate concentrations were chosen so that one experiment provided reciprocal plots for both varied substrates. All double reciprocal plots gave intersecting patterns, consistent with a sequential mechanism involving a quaternary complex with enzyme, ascorbate, ACC, and O_2. When O_2 was varied at different fixed concentrations of ACC and a constant concentration of ascorbate, the data for the $1/v$ vs $1/[O_2]$ double reciprocal plot were best fit to an equilibrium ordered pattern (intersection of the lines occurs on the *y*-axis), indicating a value of 0 for K_{ACC}/V (Figure 4a). The convergence on the *y*-intercept is indicative of a mechanism where ACC is in thermodynamic equilibrium with enzyme

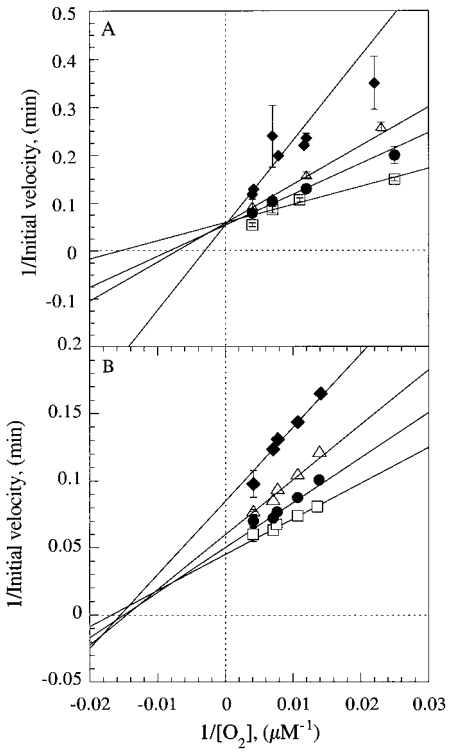

FIGURE 4: Initial velocity patterns vs O_2 concentration. (A) Conditions were constant [ascorbate] = 30 mM and 20 μM (♦), 50 μM (Δ), 75 μM (●), or 120 μM (□) ACC. (B) Conditions were constant [ACC] = 0.5 mM and 3 mM (♦), 5 mM (Δ), 8 mM (●), or 12 mM (□) ascorbate.

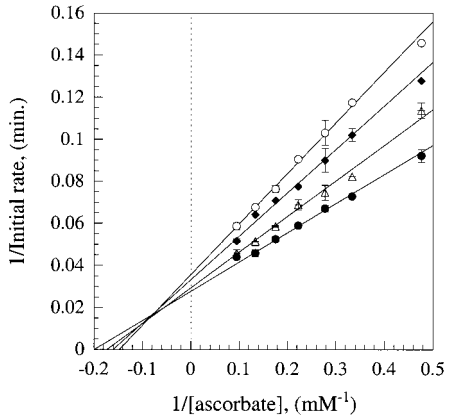

FIGURE 5: Initial velocity patterns at constant ACC concentrations. Conditions were at constant [ACC] = 0.5 mM and 102 μM (○), 132 μM (♦), 157 μM (Δ), or 258 μM (●) O_2.

and ACC binding precedes binding of O_2. The converse plot of $1/v$ vs $1/[O_2]$ at various fixed concentrations of ascorbate and a constant concentration of ACC resulted in lines that intersected to the left of the *y*-axis (Figure 4b) as did the $1/v$ versus 1/[ascorbate] double reciprocal plot at various fixed concentrations of O_2 and constant concentration of ACC (Figure 5). Since all other reciprocal plot patterns intersected to the left of the *y*-axis, no further information about the order of substrate binding can be inferred. From these data, a minimal mechanism can be described where binding of ACC and O_2 is ordered, and ascorbate can bind before ACC or after O_2.

The kinetic mechanism can be further evaluated by examining the varied substrate plots at a truly saturating concentration ($100K_m$) of the third substrate (*21*). In the case of an ordered mechanism, the second substrate to bind is identified by the substrate, which when truly saturating, gives parallel lines in the reciprocal plot. In other words, if the reversibility of the reaction between the points of addition of the variable and changing fixed substrate is broken by saturation of the remaining substrate, no slope effect will be seen in the reciprocal plot patterns (*22*). Because of an increasing background rate of oxygen consumption by the oxygen electrode in the presence of increasing concentrations of ascorbate and oxygen, conditions where ascorbate or oxygen were truly saturating were not feasible. Similarly, the apparent inhibition of ACC oxidase at high concentrations of ACC precluded the use of truly saturating concentrations of ACC for such experiments.

However, even when truly saturating concentrations cannot be attained, the slopes of the plots can still be evaluated at relatively high concentrations of the constant substrate; in this instance, the slope effect becomes progressively smaller (the lines become more parallel) as the concentration of the constant substrate is raised. Comparison of the $1/v$ vs 1/[ascorbate] reciprocal plots at various fixed O_2 concentrations and a constant ACC concentration of either 0.4 mM ($\sim 5K_m$) or 2 mM ($\sim 27K_m$) gave identical slopes (data not shown), arguing against a mechanism where ACC is the second substrate to bind in the reaction sequence.

DISCUSSION

Modified Purification and Assays using Holo-ACC Oxidase. The modified purification method described here resulted in ACC oxidase with k_{obs} from 7- to 40-fold more active than previously reported values when assayed under similar conditions (*12*, *13*). A portion of the increase in activity may be a result of separating active and inactive enzyme by using a NaCl step rather than linear gradient. Inactive enzyme is most likely a result of oxidative damage caused during purification. Varying amounts of damaged protein may accumulate depending on handling procedures throughout the purification and is likely one of the causes of the variable activity of ACC oxidase seen between our preparation and those from other laboratories, as well as from preparation to preparation within the same laboratory (*11*). However, after taking into account that active protein was ca. 75% of the total protein expressed, this would only drop our observed activity under the conditions described above from $\sim$20 to $\sim$15 min^{-1}, still up to 30-fold more active than the highest activity reported (see references above).

Two main differences in the way we have assayed ACC oxidase activity provide distinct advantages as compared to the methods used in the current literature. First, we have measured activity by monitoring oxygen consumption using a Clark-type oxygen electrode rather than ethylene production by gas chromatographic analysis. The oxygen electrode provides the ability to measure the reaction on a continuous basis, making it possible to monitor the whole reaction time course. This ensures that one is deriving rates from only the linear portion of the time course as opposed the "one time-point" assays often used, and is particularly advantageous when working at lower substrate concentrations where the rate of the reaction is more sensitive to changes in substrate concentration during the course of the reaction.

Second, we have performed a majority of our assays by initiating the reaction with ACC oxidase that has been

reconstituted with stoichiometric amounts of Fe(II) rather than by addition of ACC oxidase to a reaction mixture with excess Fe(II). The main advantage to this approach is that the iron is kept sequestered in the enzyme active site, thus minimizing the occurrence of side reactions in solution in the presence of iron, oxygen, and/or ascorbate (*23*). This approach not only diminishes the formation of damaging oxygen species due to reaction of oxygen and iron in solution, but also ensures that the ascorbate concentration is not modified either by complexation (*9*) or reaction with iron (*23*).

Iron Affinity. A growing number of non-heme iron enzymes belong to the 2H-1C iron-binding motif (4). In contrast to other heme-iron systems, many of these enzymes show characteristics consistent with rather weak iron binding. This idea is supported by the total loss of iron during purification, the rapid loss of linearity in the initial rate of the reaction when initiated with holo-enzyme, as shown here in the case of ACC oxidase (Figure 2) and with reconstituted isopenicillin N-synthase (*24*), and the high apparent K_m for iron (2 μM) determined for the 2H-1C enzyme, prolyl hydroxylase (*16*). We find a $K_d = 0.50$ μM, compared to the apparent $K_m = 5.3$ μM reported by Zhang et al. for tomato ACC oxidase (*13*) and $K_m = 40$ nm for avocado ACC oxidase (*9*). It is unclear if the ~40-fold increase in the affinity for Fe(II) is simply a function of the source of enzyme (avocado vs tomato). Previously reported apparent K_m values for Fe(II) differ 20-fold between ACC oxidase from banana [19 μM; *25*] and apple [1 μM; *15*].

We also observed inhibition in the presence of excess Fe(II); however, in our case this is seen only when high concentrations of ACC oxidase are preincubated with excess Fe(II) (Figure 1b) and not when excess Fe(II) is added to the reaction mixture (Figure 1a). The extent of inhibition (Figure 1b) may indicate a second, discrete iron-binding site. We attempted to address the question of the presence of a lower affinity allosteric binding site by performing equilibrium dialysis on a solution of high concentration of ACC oxidase preincubated with various concentrations of Fe(II), followed by analysis of iron content associated with the protein by ICP spectroscopy. However, independent of amount added, all of the iron remained in the dialysis bag with the protein. It seems likely that iron is being oxidized and precipitates in the course of the dialysis so that it cannot freely flow through the dialysis membrane. Future experiments performed in the absence of O_2 may give different results.

Rate of Fe(II) Release and the Effect of CO_2. We developed a simple method for the determination of the rate of Fe(II) release from ACC oxidase by using an alternative metal as an enzyme trap. Our data (Figure 2) indicate that Zn(II) is a specific and tight binding inhibitor of ACC oxidase and thus conducive for determination of the rate of Fe(II) release.

The absence of added bicarbonate causes a small but reproducible two-fold increase in the rate of Fe(II) release (Figure 3). It is worth mentioning that CO_2 has been found to affect the apparent K_m value of Fe(II); a K_m value of 1 μM was reported for apple ACC oxidase in the presence of saturating CO_2 (*15*), while in the absence of added CO_2, the K_m of Fe(II) decreased to a $K_m = 0.4$ μM (*26*). If an approximately similar change in K_d occurs with a change in CO_2 concentration for tomato ACC oxidase, the k_{on} for iron would increase ~4-fold with decreasing CO_2 concentration. Whether CO_2 directly interacts with the iron center has yet to be determined. It is not yet clear whether this effect has significant implications for catalysis in vivo.

Scheme 3: Steady-State Kinetic Mechanism of Tomato ACC Oxidase[a]

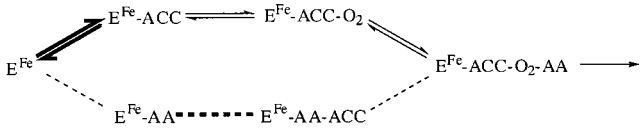

[a] The top pathway (solid arrows) is consistent with the data presented in the text. An additional pathway which can not be excluded by the data is shown below (hashed lines). Steps in thermodynamic equilibrium are shown in either bold arrows or bold hashed lines.

Kinetic Order. In this study, we have carried out initial velocity studies as a function of varying concentrations for all three substrates to determine the steady-state kinetic mechanism. The irreversibility of the reaction catalyzed by ACC oxidase precluded the use of other conventional methods such as product inhibition or isotopic exchange. Initial velocity patterns obtained with tomato ACC oxidase are consistent with a sequential mechanism involving a quaternary complex with enzyme, ascorbate, ACC, and O_2. The equilibrium ordered pattern of the $1/v$ vs $1/[O_2]$ double reciprocal plot at various fixed concentrations of ACC (Figure 4a) indicates ordered addition of ACC, in thermodynamic equilibrium with the preceding enzyme form, followed by O_2 addition. The lack of an apparent approach toward parallel velocity patterns when ACC was maintained at a high concentration relative to the K_m value precludes a strictly ordered mechanism where ACC adds as the second substrate. Thus, a mechanism consistent with the data presented is one where ACC and O_2 bind in an ordered fashion, followed by ascorbate (Scheme 3). The inability to do assays with truly saturating O_2 concentrations limits our ability to completely rule out a partially random binding mechanism in which ascorbate can also bind first, followed by ACC and O_2; we therefore also indicate the possiblity of ascorbate binding before ACC (Scheme 3).

Mechanistic Considerations and Similar Enzymes. In recent studies with avocado ACC oxidase, a random kinetic mechanism was proposed where either ACC or ascorbate binds first, followed by equilibrium ordered binding of O_2, and then ascorbate or ACC [a random A−C mechanism; *9*]. The ordered mechanism depicted in Scheme 3 requires that ACC bind at the active site before O_2 can be activated by the Fe(II) center. The key similarity between our model and the reported mechanism for avocado ACC oxidase is that the addition of a substrate always precedes binding of O_2. Such a mechanism is clearly advantageous, as the formation of oxidizing species is limited to when the relevant substrate is present, thus minimizing potential damage to the enzyme or release of strong oxidants into the cellular milieu. Consistent with this idea, EPR spectroscopy performed on avocado ACC oxidase using ACC or ACC analogues suggested that the bidentate binding of anionic ACC lowers the redox potential of the Fe(II) center, priming it for reaction with O_2 (*12*). Priming of the Fe(II) center by substrate binding appears to be an emerging theme among α-ketoglutarate-dependent and related enzymes [i.e., IPNS; *6*] and

also many other Fe(II)-enzymes, such as the phenyl-cleaving dioxygenases (reviewed in ref *27*).

EPR spectroscopic studies were unable to demonstrate the simultaneous binding of ascorbate to an enzyme−ACC−NO complex, which lead to the proposal of a ping-pong mechanism (*12*). Our kinetic data, and that of Brunhuber et al. (*9*), clearly establish a sequential mechanism. The inability to detect binding of ascorbate to the enzyme−ACC−NO complex may not be all that surprising, since ascorbate would have to perturb the metal center to cause a change in the EPR spectrum. Furthermore, the bidentate binding of ACC and a charge-transfer complex with oxygen completes the coordination sphere of the iron center (including the two histidines and aspartate that make up the active site ligands). Rather than ligation to the iron center, it is possible that ascorbate is bound in the active site by hydrogen bonding to two residues, R244 and S246 (numbering based on tomato ACC oxidase), which are conserved among both α-ketoglutarate dependent enzymes and IPNS (*28*). From the crystal structure of DAOCS with bound α-ketoglutarate, R258 and S260 hydrogen bond to the 5-carboxylate group of α-ketoglutarate (*29*). In IPNS, which uses neither ascorbate nor α-ketoglutarate, R279 and S281 are hydrogen bonded to the carboxylate of the aminoadipoyl residue of the tripeptide substrate (*30*). Although amino acid sequence similarity between ACC oxidase, IPNS, and DAOCS only approaches ∼20%, both crystal structures of DAOCS and IPNS reveal a strikingly similar jell roll motif in both structures (*29*, *30*), suggesting that ACC oxidase may also form a similar fold. Thus far, studies have not been reported exploring the effects of mutations of these two residues on the kinetic parameters for ACC oxidase.

APPENDIX

Derivation of Equation 2. In the titration of enzyme with iron, there are conditions where [ACC oxidase] is higher than $[Fe(II)]_{total}$. Therefore, the assumption that $[Fe(II)]_{free}$ can be approximated by $[Fe(II)]_{total}$ is no longer correct. The rate expression as a function of free metal follows, where $[M]_f$ represents the $[Fe(II)]_{free}$:

$$v = \frac{V_{max}}{1 + \frac{K_d}{[M]_f}} \tag{A1}$$

$[M]_f$ can be expressed in terms of total metal, $[M]_t$, and enzyme-bound metal, [EM]. Likewise, a conservation equation can be written for the concentration of free enzyme, $[E]_f$:

$$[M]_f = [M]_t - [EM] \tag{A2}$$

$$[E]_f = [E]_t - [EM] \tag{A3}$$

Equation A2 is substituted into eq A1 to give a rate expression in terms of the known quantity, $[M]_t$, but then the quantity [EM] must also be known. [EM] can be expressed in terms of the dissociation constant, as follows:

$$[EM] = \frac{[E]_f[M]_f}{K_d} \tag{A4}$$

Substitution of eqs A2 and A3 into A4 results in the following expression for [EM]:

$$[EM] = \frac{[E]_t[M]_t - [EM][M]_t - [EM][E]_t + [EM]^2}{K_d} \tag{A5}$$

The quantity [EM] is solved by using the quadratic equation, where only the minus value of the solution needs to be considered.

$$[EM] = (K_d + [M]_t + [E]_t) - \frac{\sqrt{(-K_d - [M]_t - [E]_t)^2 - 4[E]_t[M]_t}}{2} \tag{A6}$$

Equation A6 is substituted into eq A1, which gives rise to eq 2 in the text.

REFERENCES

1. Bleecker, A. B. (1999) *Trends Plant Sci. 4*, 269−274.
2. Peiser, G. D., Wang, T.-T., Hoffman, N. E., Yang, S. F., Liu, H.-W., and Walsh, C. T. (1984) *Proc. Natl. Acad. Sci. U.S.A. 81*, 3059−3063.
3. Dong, J. G., Fernandez-Maculet, J. C., and Yang, S. F. (1992) *Proc. Natl. Acad. Sci. U.S.A. 89*, 9789−9793.
4. Hegg, E.L and Que, L. Jr. (1997) *Eur. J. Biochem. 250*, 625−629.
5. Kivirikko, K. I. (1989) *FASEB J. 3*, 1609−1617.
6. Baldwin, J. E. and Bradley, M. (1990) *Chem. Rev. 90*, 1079−1088.
7. Baldwin, J. E., Adlington, R. M., Schofield, C. J., Sobey, W. J. and Wood, M. E. (1989) *J. Chem. Soc., Chem. Commun.* 1012−1015.
8. Elson, S. W., Baggaley, K. H., Gillett, J., Holland, S., Nicholson, N. H., Sime, J. T., and Woroniecki, S. R. (1987) *J. Chem. Soc., Chem. Commun.* 1736−1738.
9. Brunhuber, N. M. W., Mort, J. L., Christoffersen, R. E., and Reich, N. O. (2000) *Biochemistry 39*, 10730−10738.
10. Hamilton, A. J., Bouzayen, M., and Grierson, D. (1991) *Proc. Natl. Acad. Sci. U.S.A. 88*, 7434−7437.
11. Barlow, J. N., Zhang, Z., John, P., Baldwin, J. E., and Schofield, C. J. (1997) *Biochemistry 36*, 3563−3569.
12. Rocklin, A. M., Tierney, D. L., Kofman, V., Brunhuber, N. M. W., Hoffman, F. M., Christoffersen, R. E., Reich, N. O., Lipscomb, J. D., and Que, L., Jr. (1999) *Proc. Natl. Acad. Sci. U.S.A. 96*, 7905−7909.
13. Zhang, Z., Schofield, C. J., Baldwin, J. E., Thomas, P., and John, P. (1995) *Biochem. J. 307*, 77−85.
14. McGarvey, D. J. and Christoffersen, R. E. (1992) *J. Biol. Chem. 267*, 5964−5967.
15. Pirrung, M. C., Kaiser, L. M., and Chen, J. (1993) *Biochemistry 32*, 7445−7450.
16. Myllyharju, J. and Kivirikko, K. I. (1997) *EMBO J. 16*, 1173−1180.
17. Dong, J. G., Fernández-Maculet, J. C., and Yang, S. F. (1992) *Proc. Natl. Acad. Sci. U.S.A. 89*, 9789−9793.
18. Fernández-Maculet, J. C., Dong, J. G., and Yang, S. F (1993) *Biochem. Biophys. Res. Commun. 193*, 1168−1173.
19. Zhang, Z., Barlow, J. N., Baldwin, J. E., and Schofield, C. J. (1997) *Biochemistry 36*, 15999−16007.
20. Smith, J. J., Ververidis, P., and John, P. (1993) *Phytochem. 32*, 1381−1386.
21. Viola, R. E. and Cleland, W. W. (1982) *Methods Enzymol. 87*, 353−366.
22. Cleland, W. W. (1992) *The Enzymes 19*, 99−158.
23. Martell, A. E. (1982) in *Ascorbic Acid: Chemistry, Metabolism, and Uses* (Seib, P. A., and Tolbert, B. M., Eds.) pp 153−178, American Chemical Society, Washington, D. C.

24. Kriauciunas, A., Frolik, C. A., Hassell, R. C., Skatrud, P. L., Johnson, M. G., Holbrook, N. L., and Chen, V. J. (1991) *J. Biol. Chem. 266*, 11779−11788.
25. Moya-Leon, M. A., and John, P. (1995) *Phytochem. 39*, 15−20.
26. Dupille, E., Rombaldi, C., Lelievre, J.-M., Cleyet-Marcel, J. C., Pech, J.-C., and Latche, A. (1993) *Planta 190*, 65−70.
27. Que, L., Jr., and Ho, R. Y. N. (1996) *Chem. Rev. 96*, 2607−2624.
28. Borovok, I., Landman, O., Kreisberg-Zakarin, R., Aharonowitz, Y., and Cohen, G. (1996) *Biochemistry 35*, 1981−1987.
29. Valegård, K., Terwisscha van Scheltinga, A. C., Lloyd, M. D., Hara, T., Ramaswamy, S., Perrakis, A., Thompson, A., Lee, H.-J., Baldwin, J. E., Schofield, C. J., Hajdu, J., and Andersson, I (1998) *Nature 394*, 805−809.
30. Roach, P. L., Clifton, I. J., Hensgens, C. M. H., Shibata, N., Schofield, C. J., Hajdu, J., and Baldwin, J. E. (1997) *Nature 387*, 827−830.

BI010329C